18

Institute of Theoretical
and Experimental Physics

FERMILAB

46-00

MAR 2 2 2001

LIBRARY

A. Akindinov, V. Golovine, Yu. Kiselev,
A. Martemianov, V. Petrov, V. Plotnikov,
V. Sheinkman, A. Smirnitski, V. Ushakov,
K. Voloshin

Dup

Multi-Gap DRPC Performance for Time-of-Flight Measurements

Fermilab Library
0 1160 0089674

Moscow 2000

UDK 539.1 M-16

MULTI-GAP DRPC PERFORMANCE FOR TIME-OF-FLIGHT MEASUREMENTS: Preprint ITEP 46-00/

A. Akindinov, V. Golovine, Yu. Kiselev, A. Martemianov, V. Petrov, V. Plotnikov, V. Sheinkman, A. Smirnitski, V. Ushakov, K. Voloshin - M., 2000 - 16p.

Described are the first data on the possibilities of a new detector of ionising particles, a Dielectric Resistive Plate Chamber (DRPC), intented to be used in precise time-of-flight measurements

A multilayer detector design (with 2–4 gas gaps) shows characteristics, including timing properties, close to those of the traditional technology based on scintillators and photomultipliers. The channel price in the DRPC case appears to be an order of magnitude less.

The results declare that a new promising technology for time-of-flight measurements has been invented.

Приведены первые данные о возможностях нового детектора ионизующих частиц — диэлектрически-резистивной плоско-параллельной камеры (ДРПК) — для прецизионного измерения времени пролета.

В многослойном варианте (2–4 газовых слоя) характеристики детектора, включая временное разрешение, достигают уровня лучших образцов традиционной технологии, основанной на сцинтилляторах и фотоумножителях. При этом стоимость канала оказывается на порядок меньшей.

Результаты позволяют сделать вывод об открытиии новой перспективной технологии измерения времени пролета.

Fig. - 19, ref. - 5 name.

© Институт теоретической и экспериментальной физики, 2000

A copy of this preprint is available on the Web at
http://triton.itep.ru/kl/ITEP-ALICE/ITEP4600/ITEP4600.html

1. Detector Description

1.1. Principles of Operation and Construction

In 1997–1999 the first beam test results with a new gaseous detector for time-of-flight (TOF) measurements, Dielectric Resistive Plate Chamber (DRPC), were obtained in the slopes of an R&D program for TOF gaseous detectors proposed to be used in future experiments on high energy nuclear collisions at BNL and LHC.

Starting from 1999, the R&D was supported from RFBR grant # 99–02–18377.

DRPC [1] was being developed as a frontier detector between PPC and RPC, in order to avoid large energy resolution in spark cases (RPC feature), keeping high time resolution altogether with fast response, shown in previous experiments with PPC [2]. A dielectric layer introduced between the electrodes is covered with a surfacial resistivity on the gas side, allowing, in case of a breakdown, to decrease or limit the spark energy by charging an elementary plate condensator, which then discharges through the resistive surface. The detector has shown stability of operation in the avalanche mode within a wide range of applied voltages. Time response and energy resolution in spark events may be adjusted by varying the main electric parameters of the detector: dielectric layer capacity and surfacial resistance.

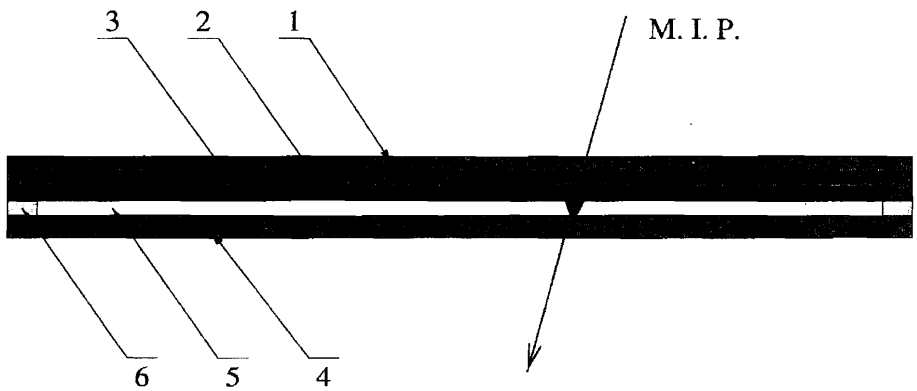

Fig. 1. DRPC construction: 1 — conducting layer, 2 — dielectric, 3 — resistive layer, 4 — external electrode, 5 — gas gap, 6 — spacers.

The basic detector construction used in the tests is shown in Fig. 1. A plate condensator, several milimeters thick, has external dimensions 50×50 mm^2. One of the electrodes is made of a conducting material, the other has a resistance-dielectric-metal layer structure. The 0.6 mm gas gap was chosen basing on PPC experience as providing high registration efficiency for MIP altogether with a rather good time resolution, and is supported by means of ceramic spacers. Accuracy requirements are the same as in the traditional PPC: the electrodes and spacers are kept flat and parallel within the several micrometers accuracy.

The layer electrode is a crucial part of the detector. The dielectric thickness d_d is determined from the condition $d_d \leq \epsilon_d \cdot d_g/\epsilon_g$, where d_g is the gas gap width, ϵ_d and ϵ_g are the dielectric and gas dielectricities correspondently. We used 1 mm thick Al_2O_3 with $\epsilon/\epsilon_{air} \approx 10$. The dielectric was covered with a thin layer of resistive material SiC or TiC having volume

resistivity $\rho = 10^2 - 10^3\ \Omega \cdot \mathrm{cm}$. The outer side of this electrode is metallized through evaporation and actually operates as the second condensator electrode, producing the electric field responsible for gas amplification.

In the tests, double-gap detectors formed of two adequate single gaps were investigated.

1.2. Limited Energy Resolution in Breakdowns

It has been known so far that one of the main disadvantages of PPC is its high energy resolution during spontaneous breakdowns, which is limited only by energy acquired during the discharge. Despite the very low probability of such a breakdown (10^{-6} if modern freon-based gases are involved), the energy resolution is six orders of magnitude higher than in ordinal avalanche cases. Besides harming the detector and electronics, such a huge energy resolution leads to *cross-talks* between different cells of the large module and to a large *dead time* of the detector after breakdowns.

DRPC was suggested as a principal solution in the task of suppressing the energy resolution during breakdowns.

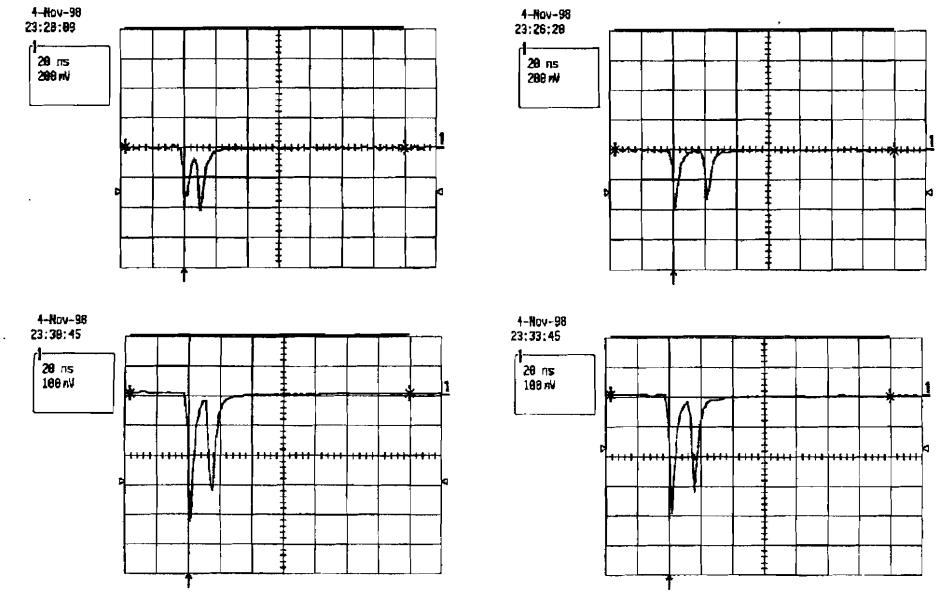

Fig. 2. Oscillograms of breakdown signals measured directly from the detector with 50 Ω output resistance.

Oscillograms in Fig. 2 show breakdown signals from DRPC without further amplification measured on a 50 Ω resistance at the output. Signal shapes have two bumps (seen with PPC as well), very short total duration of about 20 ns, and small amplitudes of 100–200 mV.

Summarised energy resolution is of the order of 1 nC which is two orders of magnitude lower than in a similar PPC case.

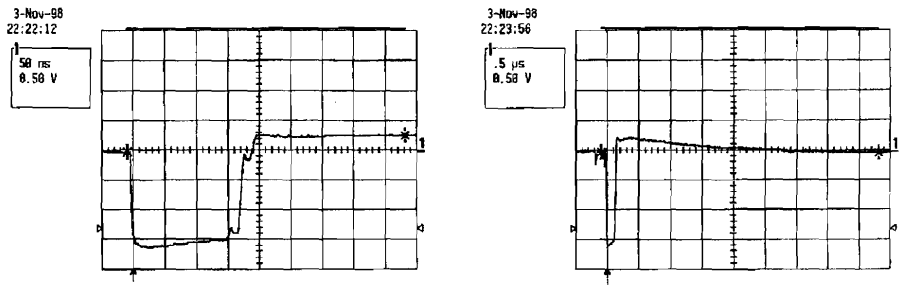

Fig. 3. Oscillograms of fast electronics response for breakdown signals.

Fig. 3 represents the reaction of fast sensitive electronics on such a limited breakdown signal. One can see that the amplifier becomes saturated, but only for a short time period of about 200 ns which cannot influence the total *dead time* of the detector.

1.3. Admixture of Streamer Signals

As in the PPC case, the avalanche evolution inside DRPC may lead to a streamer formation. The streamer probability depends primarily on the chosen gas and may be either strongly suppressed or released to let the detector work in the streamer mode.

A small admixture of streamer signals rising to a 10^{-2} level at the end of the counting plateau has been seen, with DME + CF_3Br as a working gas.

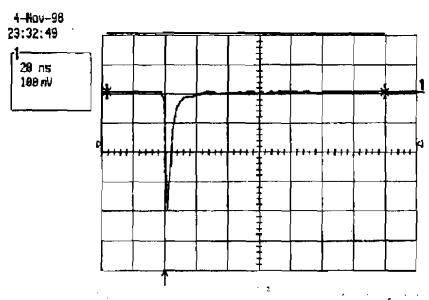

Fig. 4. Oscillogram of a single streamer signal.

The oscillogram in Fig. 4 shows the single streamer signal from DRPC without amplification.

All streamer signals have same shapes with fast rise times and large amplitudes. Such working regime seems to be very attractive and must be additionally investigated.

1.4. Multi-Gap DRPC

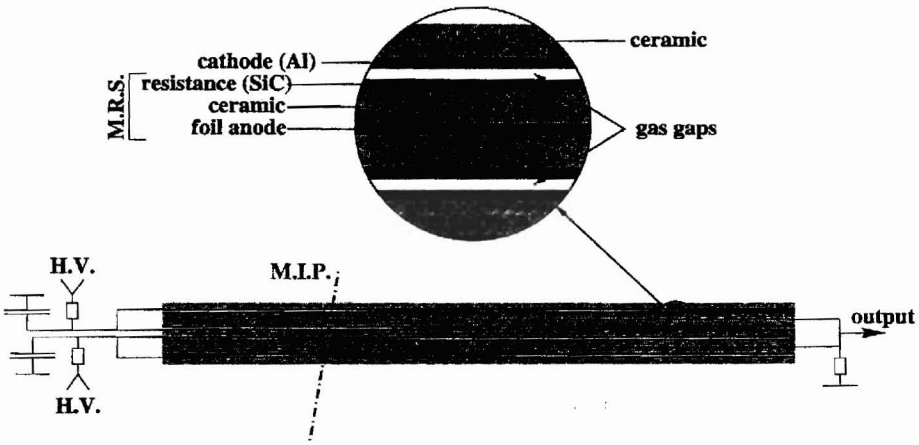

Fig. 5. Four-gap DRPC construction.

A detector which timing characteristics are currently under investigation is schematically shown in Fig. 5. A four-gap DRPC consists of several ceramic plates (0.5 mm of ordinary unpolished ceramics) which form the gas gaps, each 0.3 mm wide. As was expected, decreasing the gap width rises the time resolution. The number of gaps (2 in previous version) was doubled to keep the MIP registration efficiency close to 100%.

The chamber is formed of two types of electrodes. Ceramic cathodes are metallised with aluminium. Dielectric-resistive electrodes are also made of ceramics metallised with aluminum on the one side and covered through evaporation with semi-conducting SiC on the other. The plates are assembled in pairs so that the metal layer, common among the two gaps, is inside, and the semi-conducting layers are on the gas sides. The idea of electrical connection between the semi-conductor and the metal is described in [3]. The detector has a square working surface 2×2 cm^2.

2. DRPC Cell Performance

2.1. Beam Test Setups at CERN and ITEP

DRPC has been studied as a detector for high precision and efficient time measurements on PS beams at ITEP and CERN. π^--beams, with 2–7 GeV/c momenta, 100–10^5 s^{-1} intensities, and several cm^2 cross-section at the detector position, were usually used.

Trigger and start counters, made of scintillators of different sizes and modifications, and adapted for time measurements, were positioned on the same beam. The trigger consisted of 6 to 10 counters, including those situated on precise movable platforms, which determined the space position of the beam before and after the target, for efficiency measurements, as

well as the place where the beam crossed the detector plane. Time measurement scheme included 2 start scintillator counters (each with 2 PMs), it was always possible to check the time resolution of these counters on-line during the data acquisition. The typical resolution of the start system was 150 ps.

The signal from the detector was used as the *stop* in the scheme. The resolution of start counters was quadratically subtracted from the resolution of MIP's time of flight along a fixed base, resulting in the detector resolution.

All the electronics for trigger and timing measurements were assembled in the NIM and CAMAC standards.

Specially designed fast and low-noise electronics, consisting of a preamplifier, a main amplifier and a discriminator, were used for registration of signals from the gaseous detector. The scheme comes as a further development of ideas described in [4].

Various gas mixtures based on either DME or different types of freons with normal quality, were used as working gases in the detector. A simple gas system allowed to mix gases at rather small fluxes of up to several litres per hour. No special control of quality and other gas parameters was undertaken.

DME + 5%CF_3Br was most thoroughly studied as a working gas for DRPC. The best results were obtained with $C_2H_2F_4$ + 15%DME and $C_2H_2F_4$ + 5%iso-C_4H_{10} + 10%SF_6.

2.2. Double-Gap DRPC with 0.6 mm Gaps

Fig. 6 represents the typical result of the DRPC efficiency and time resolution measurements.

Plot in Fig. 6*a* shows the amplitude distribution measured with ADC. A very narrow pedestal, corresponding to noise characteristics of both the detector and the electronic channel, may be clearly seen. Efficient signals have a wide non-exponential distribution. Such a shape allows to achieve high efficiency (98% in this particular case) even if the detecting threshold of the electronics is high.

Distribution of *start* minus *stop* time versus amplitudes is shown in Fig. 6*b*. One can clearly see that the mean time changes as amplitude increases for about 1 ns (the value must correspond to the signal rise time), since a constant threshold discriminator produces different times for jitters having different amplitudes. The solid line shows an approximation used for fitting this correlation.

Taking into account T(A) dependence leads to the time resolution being dependent on amplitudes in the way presented in Fig. 6*c*. It may be seen that the time resolution is close or even better than 200 ps in a wide range of amplitudes, excluding the lower region close to discriminator threshold of 15 mV.

Finally, the DRPC time resolution at a fixed efficiency is shown in Fig. 6*d*. Better than 200 ps time resolution may be reached at a high registration efficiency (95% in this case).

All the data shown in Fig. 6 were obtained at a fixed high voltage applied to the chamber. The fact that the time resolution does not depend on the applied voltage and the discriminator threshold in their wide ranges is demonstrated in Fig. 7. Amplitude distributions and timing characteristics are plotted for several values of applied voltages starting from 3.7 kV with 100 V increment from plot to plot. Time resolution remains almost the same at different voltages (0.5 kV plateau) and approximately equals to 200 ps. The detector efficiency stays high as well.

DRPC time resolution of 200 ps is close to the same value measured for PPC with 0.6 mm gas gaps. It has been seen that the PPC time resolution decreases approximately in a linear

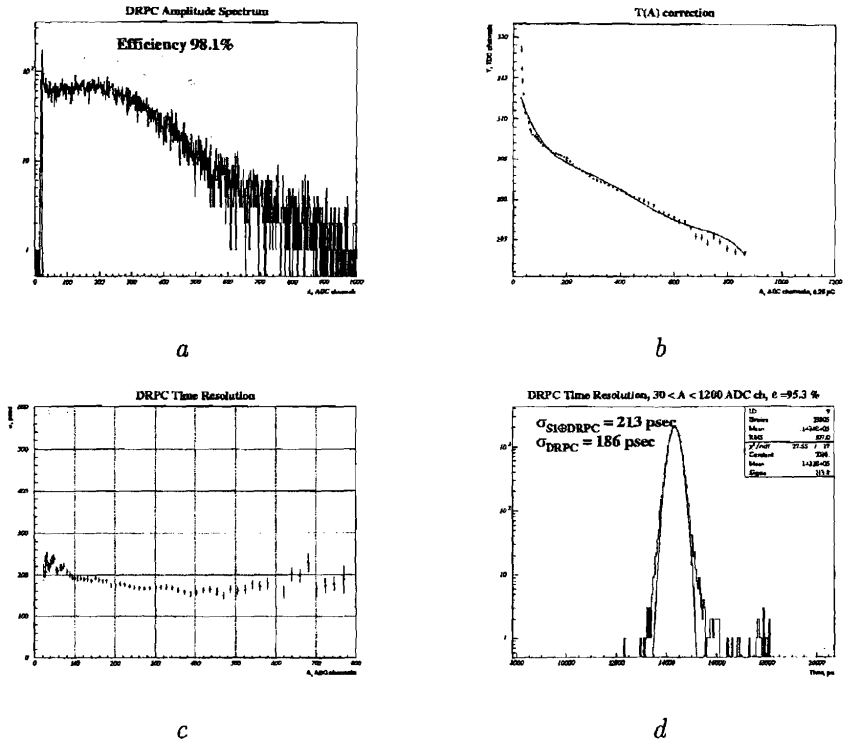

Fig. 6. Results of time resolution and efficiency measurements for double-gap DRPC: *a* — amplitude spectrum, 98.1% of events lie out of the pedestal bump, *b* — polynom T(A) correction, *c* — time resolution at different amplitudes, *d* — total time resolution, σ_{DRPC} stays for what is left after subtraction of start resolution.

way as the gap becomes narrower, and 0.6 mm is a minimal value still giving high efficiency of MIP registration with double-gap detectors. In this sense, one can expect that, similar to PPC, the DRPC time resolution of 200 ps may be significantly improved by decreasing the gap width.

2.3. Four-Gap DRPC with 0.3 mm Gaps

Methodics used in time-of-flight resolution and registration efficiency measurements, involving four-gap DRPC, slightly differs of that described in [3]. The same specially designed front-end electronics and the same gas mixture 85%$C_2H_2F_4$ + 5%iso-C_4H_{10} + 10%SF_6 were used. The start part of the setup, based on scintillator counters, was modified and allowed to analyze information from several detectors simultaneously.

The counting rate, or particle flux over the working surface, is an important parame-

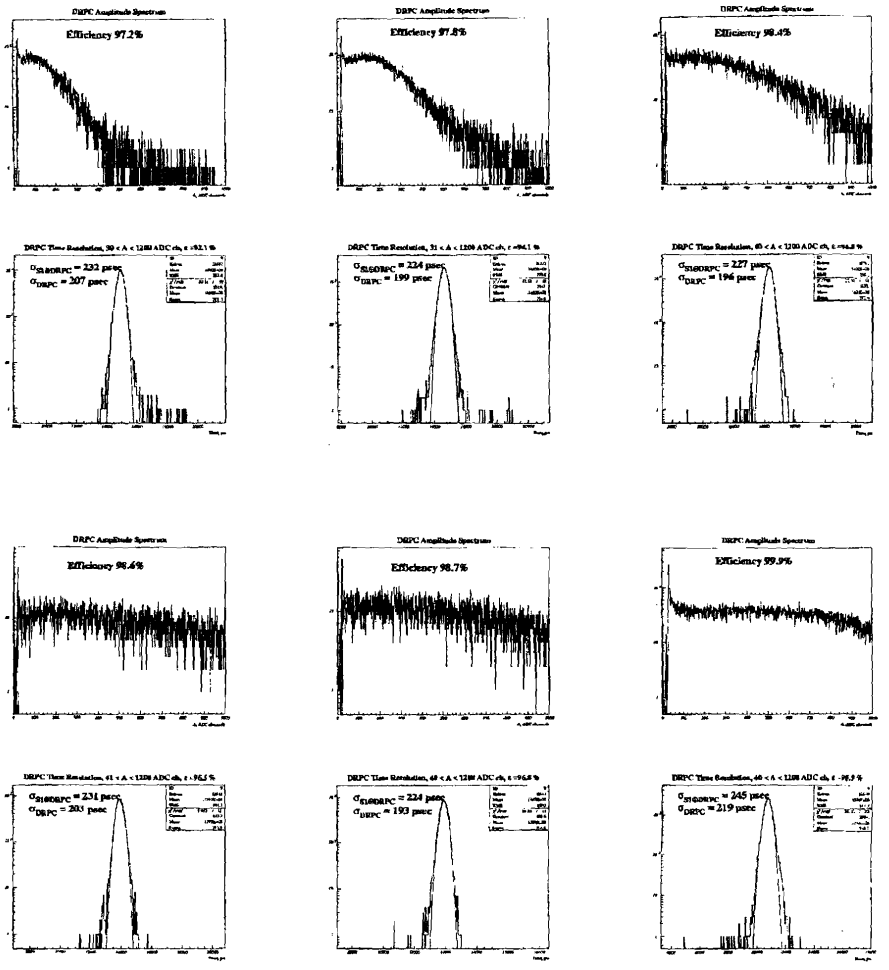

Fig. 7. Time resolution and efficiency measurements under different applied voltages (100 V high voltage increment from plot to plot).

ter of the described detector type. During the measurements, it was fixed at the level of 1 kHz·s^{-1}·cm^{-2}, which is higher than, for instance, in the ALICE conditions (100–200 Hz·s^{-1}·cm^{-2}). Special measurements were performed to study how the rate influences the detector resolution.

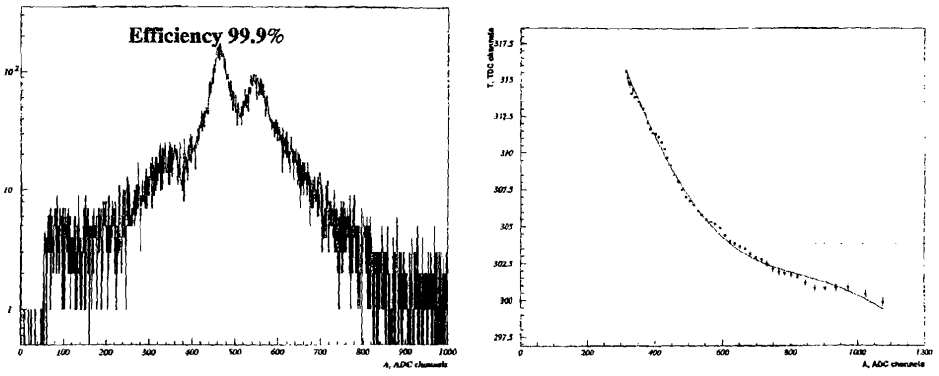

a *b*

Fig. 8. DRPC amplitude spectrum (*a*) and corresponding polynomial T(A)-correction (*b*).

The amplitude spectrum from the amplifier output is shown in Fig. 8*a*. More specifically, it shows the charge integrated by a charge-sensitive ADC. Although the front-end electronics is not linear in the whole range of amplitudes, it may be clearly seen that the amplitude spectrum shape has a peak, staying far from the pedestal on a slightly changing background. Such amplitudes correspond to a gas amplification of 10^7 and allow to obtain excellent registration efficiency at different high voltages and high discriminator thresholds.

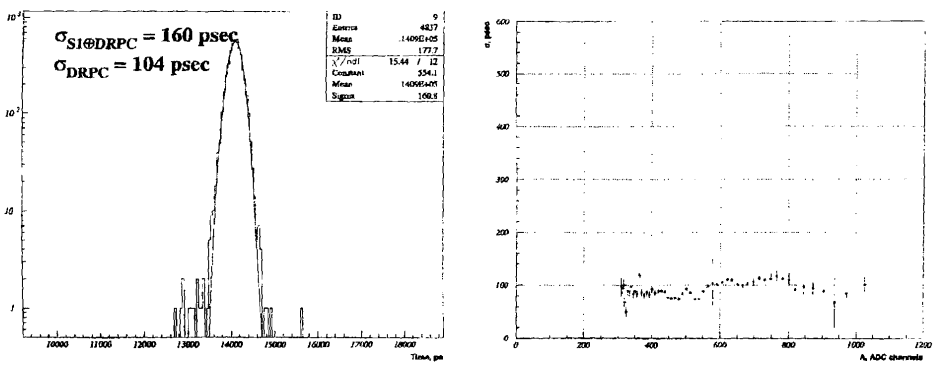

a *b*

Fig. 9. DRPC time resolution: *a* — at different amplitude ranges, *b* — total.

A typical time-of-flight distribution, summarised over the whole range of amplitudes, with the total registration efficiency close to 95%, is shown in Fig. 9*a*. One can see that the

standard deviation is really on the level of 100 ps, and the distribution has very unsignificant *tails*. Fig. 9*b* represents the same data in more details: time resolution is shown for different amplitudes in their whole range. The dependence is very slight and can be hardly seen, the resolution is close to 100 ps at all the amplitudes, thus explaining the *tails* absence in Fig. 9*a*.

The amplitude distribution represented in Fig. 8*a* has a clear peak but is significantly wide at its basement. To obtain high efficiency in the whole amplitude range, while measuring the time with a constant threshold discriminator (CTD), an amplitude correction must be performed. Fig. 8*b* shows the dependence of the CTD trigger on the signal amplitude, as well as the applied polynomial T(A)-correction. The smooth curve covers an approximately 2 ns range in time.

2.4. Miscallenious Parameters: High Voltage, Discriminator Threshold, etc.

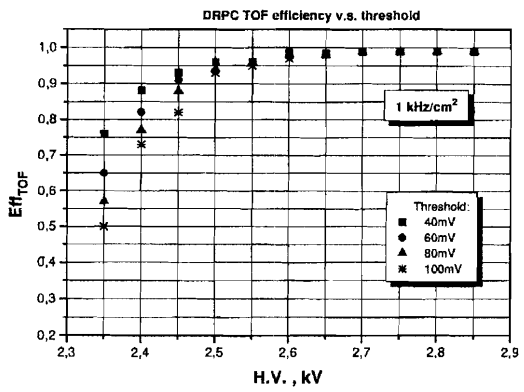

Fig. 10. DRPC registration efficiency for different high voltages and discriminator thresholds.

Both the MIP registration efficiency and the DRPC time resolution do not depend on the applied high voltage and the CTD threshold in their wide range. Fig. 10 shows how the efficiency depends on the high voltage at different discriminator thresholds (40–100 mV). One can see that there exists a plateau, more than 200 mV wide, on which the efficiency is very close to 100%. At the voltages lower than 2.5–2.6 kV, a dependence of efficiency on the discriminator threshold becomes visible.

The time resolution σ_{TOF} is influenced by the high voltage and the discriminator threshold in a way shown in Fig. 11. Increasing the high voltage from 2.3 kV to 2.5 kV leads to the σ_{TOF} decrease from 200 ps to 100 ps which then stays constant till 2.8 kV, i.e. inside a 300 V-wide high voltage range. Changing the threshold from 40 mV to 120 mV does not influence the time resolution.

All the described data were obtained at a fixed counting rate of 1 kHz$\cdot$s$^{-1}\times$ cm^{-2}. Fig. 12 shows a dependence of the TOF resolution on the particle flux at a 40 mV discriminator

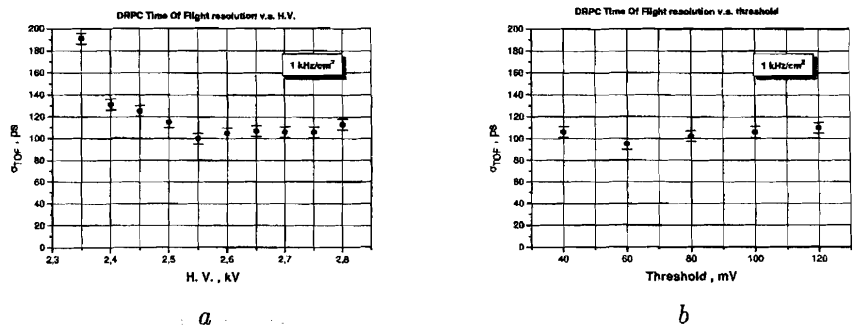

Fig. 11. DRPC time-of-flight resolution at different high voltages *(a)* and discriminator thresholds *(b)*.

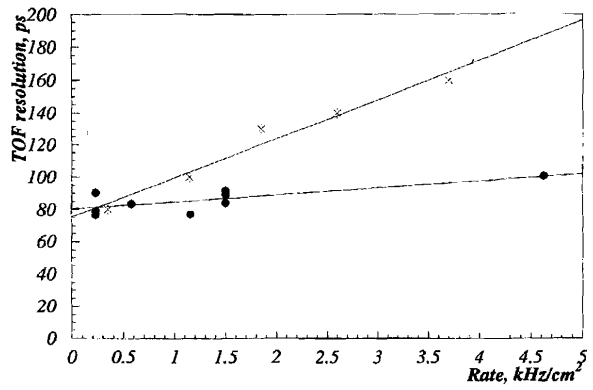

Fig. 12. DRPC TOF resolution for different counting rates. Stars and circles stay correspondently for previous and modern DRPC designs.

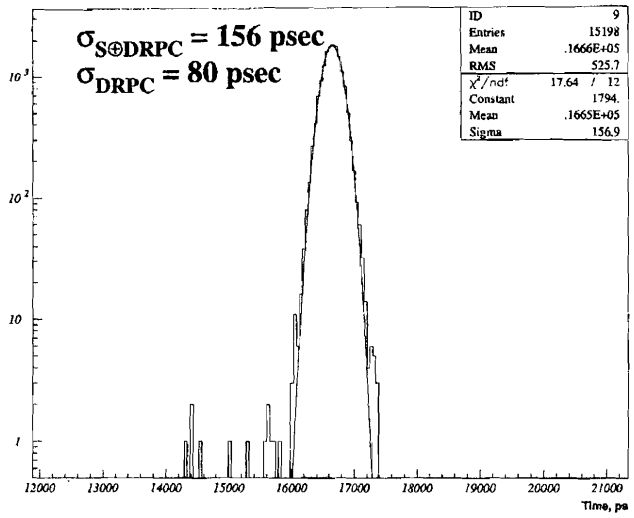

Fig. 13. DRPC TOF resolution at low counting rate.

threshold. The stars on the plot correspond to the initial version of the detector described in [5], in which the resolution grows almost linearly and reaches 150 ps at 4 kHz·s^{-1}·cm^{-2}. For the updated version of the detector, which does not have an additional resistivity between the working surface and metal connectors, the dependence of the resolution on the rate is much less: the circles in Fig. 12 show that the σ_{TOF} stays approximately constant within a 100 ps limit up to a 4.5 kHz·s^{-1}·cm^{-2} counting rate. In both detector versions the resolution is better than 100 ps at 0.5 kHz·s^{-1}·cm^{-2} (see Fig. 13).

2.5. *Tails* in TOF Spectrum

It is well known that for the PID performance of a TOF detector, the so-called *tails* in timing spectra are a question of crucial importance. The problem becomes even more important in a case when PID by TOF is made for particles with significantly different yields. For instance, a comparatively small amount of kaons produced in nuclear collisions cannot be distinguished from a background of *tails* left by a much more abundant pion spectrum. This problem had been under investigation for several years, in concern with Pestov spark counters (in which *tails* are originated by delayed sparks), and PPCs (where *tails* occur due to time jitter being dependent on signal amplitudes).

Tails admixture in DRPC TOF spectra was estimated by using a double-Gaussian fit. Fig. 14 shows an example of DRPC TOF distribution. A usual Gaussian fit gives an 85 ps time resolution (after quadratical subtraction of the start counters resolution), with a small admixture of *tails* on both sides of the spectra. Fitting the same data with two independent Gaussian curves allows to conclude that the main signal with a 74 ps sigma lies on a 9% admixture of background signals with a 250 ps-wide distribution. The level of *tails* thus

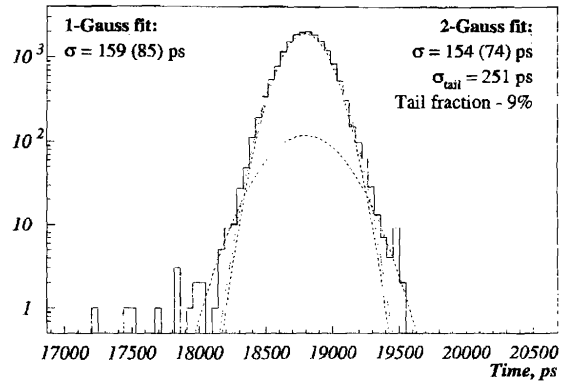

Fig. 14. TOF resolution of DRPC. Numbers in brackets show sigma after subtraction of the start counter resolution. Double-Gauss method allows to estimate tails fraction in the time resolution of the detector.

appears to be much less than in the case of Pestov counters. *Tails'* nature is still unknown and is subject for further investigation.

2.6. PID Performance by DRPC under the ALICE Conditions

PID performance by DRPC, with a natural admixture of *tails* in the timing spectra of the detector, was studied experimentally at the ITEP PS. The beam was constituted of different sorts of particles (π, K, p, d), which quantities could be varied. An excellent PID was performed by means of a long-base TOF system and a system of gaseous Čerenkov counters, established on the beam line. These facilities allowed to know the sort of each beam particle in advance, before DRPC TOF measurements, and thus to check the quality of PID performed by DRPC.

Fig. 15 shows a T–A distribution of π and K events in DRPC. The beam momentum (1.3 GeV/c), the TOF base length (3.8 m) and the K admixture into π events (10%) were chosen in accordance with the ALICE conditions. One can see that π and K events are clearly separated, and a gap between two regions can be evidently observed.

A quantitive result of the separation is presented in Fig. 16. The main part of the plot shows two peaks in the timing spectrum corresponding to π and K, after T(A)-correction applied to the whole data. Since the sorts of particles were reliably known in advance, pions and kaons were distinguished even in the intermediate region. Both peaks were approximated with 2 Gaussian distributions. The time resolution for pions is 89 ps, 8%-*tails* are 260 ps wide. The kaons time resolution is 82 ps, 9%-*tails* are 270 ps wide. Fig. 16 illustrates how crucial *tails* are in the task of PID; were if not for them, the spectrum would be described only by single Gaussian fits, and an unmistakable separation could be done almost everywhere. In reality, presence of K's in π's distribution is low, while π's contamination into K's may be significant,

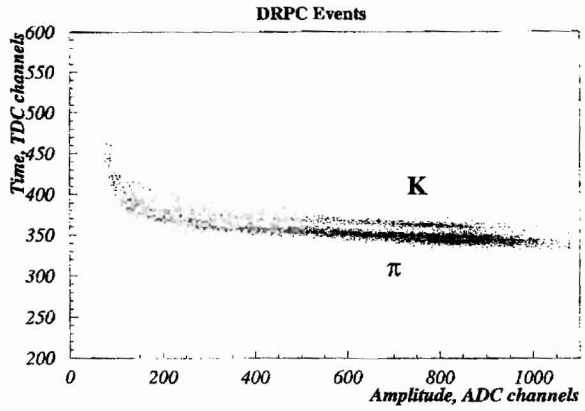

Fig. 15. π and K events in DRPC at $p = 1.3$ GeV/c and $l = 3.8$ m (ALICE conditions).

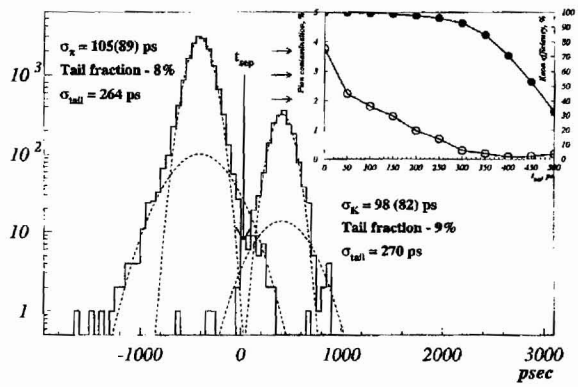

Fig. 16. π/K separation by means of DRPC-based TOF at $p = 1.3$ GeV/c. π contamination and K registration efficiency depending on TOF separating parameter are shown in the top right corner.

depending on a cut parameter t_{sep}. Shifting t_{sep} to higher times leads to less contamination on the one hand, but to less K's registration efficiency on the other. Plot in the right upper corner of Fig. 16 demonstrates this conclusion quantitively. In the middle position, where the peaks intersect, the registration efficiency of kaons is close to 100%, the pion contamination is about 4%. Moving to upper t_{sep} decreases the contamination rapidly, which reaches 1% at 95% of K efficiency, and almost disappears at 90% of K efficiency.

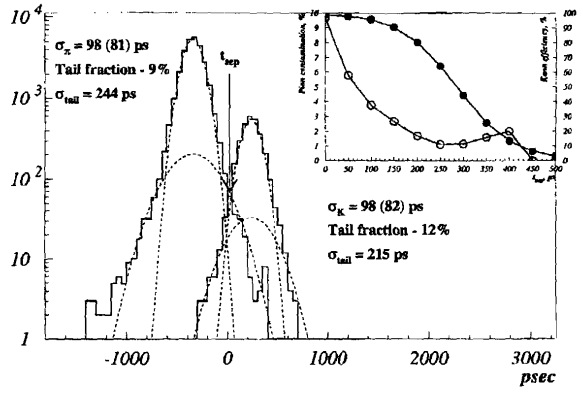

Fig. 17. π/K separation by means of DRPC-based TOF at $p = 1.5$ GeV/c. π contamination and K registration efficiency depending on TOF separating parameter are shown in the top right corner.

Fig. 17 shows similar results for a 1.5 GeV/c momentum, which is supposed to be a limit for reliable π and K separation in ALICE. At 100% of K registration efficiency, the π contamination equals to 10%, then it decreases to several percent at 90% of K efficiency. It is seen that even in this most critical case, the contamination of π's into K's, caused by *tails*, still stays on a few percent level, leaving the K registration efficiency rather high.

The conclusion is that the *tails* admixture in the DRPC TOF spectrum does not change significantly the PID performance of the ALICE TOF detector. For comparison, the income into the same contamination parameter, produced by track extrapolation from TPC to TOF on a length of 1 m, taking into account rescattering processes, is not less than 10% (see ALICE PID notes for details).

2.7. DRPC Performance for Particles with Different Ionising Properties

DRPC response to ionising particles with different dE/dx was also studied during the beam tests. Fig. 18 shows T–A events in DRPC, measured with beam of two different momenta, and constituted of π, p and d. The separation quality may be visually observed. It may also be seen that increasing of dE/dx up to about 2 MIPs (look at the deutron events) makes the

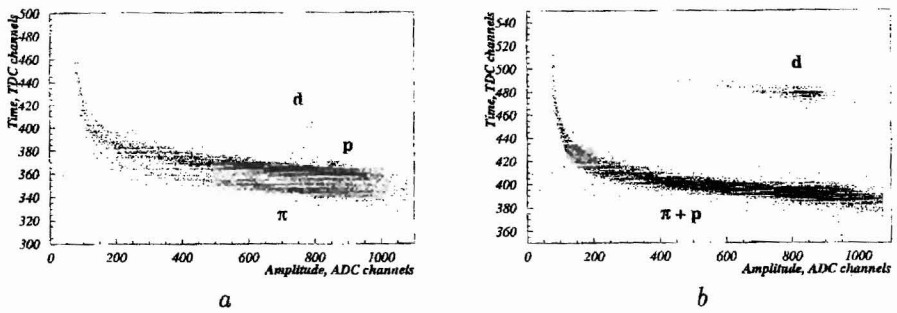

Fig. 18. Positive beam data obtained with DRPC at $p = 2.25$ GeV/c (a) and $p = 1.5$ GeV/c (b).

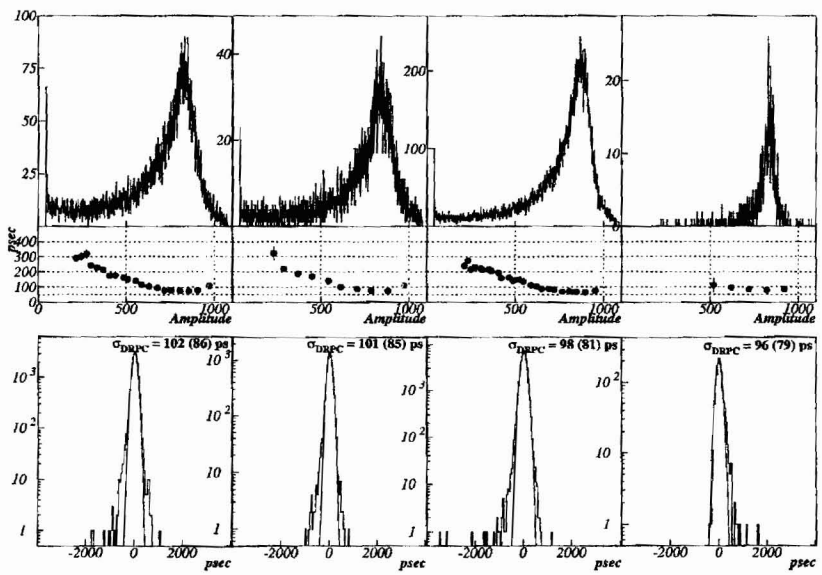

Fig. 19. Amplitude spectra, amplitude dependences of time resolution and total time resolutions measured with DRPC for different ionizing particles. dE/dx increases from left to right.

T(A)-dependence almost linear, with a very slight change along the T-axis, which simplifies the procedure of T(A)-correction.

Amplitude spectra and TOF resolutions are shown in Fig. 19 for protons with $p = 2.25$ GeV/c, pions with $p = 2.25$ GeV/c, protons with $p = 1.5$ GeV/c, and deutrons with $p = 1.5$ GeV/c. The corresponding values of dE/dx in MIP units are: 1, 1.1, 1.2, and 2.2. The shown results were measured with modified front-end electronics. All the amplitude spectra have peaks, staying far apart from the pedestals on small background basements, the value of background decreasing at higher dE/dx. TOF resolutions, calculated with single Gaussian fits, are about 80 ps in all the cases.

The R&D on the new TOF technology was performed with a support from RFBR grant # 99–02–18377.

References

[1] V. Golovine, A. Smirnitski. Patent of Russia #2148283, priority of 13.11.1998.

[2] V. Akimov *et al.* Nucl. Instrum. Methods **A344** (1994) 120.

[3] A. Akindinov *et al.* Preprint ITEP 45–98, 1998.

[4] R. D'Alessandro *et al.* Preprint ITEP 51–95, 1995.
A. Martemianov. Proc. of the 1st workshop on electronics for LHC experiments, Lisbon, 11–15 Sept., 1995.

[5] A. Akindinov *et al.* Preprint ITEP 20–99, 1999.

А. Акиндинов, В. Головин и др.
Многозазорная диэлектрически-резистивная камера для времяпролетных измерений.

Подписано к печати 28.12.00 Формат 60×90 1/16
Усл.-печ.л. 1,0 Уч.-изд.л. 0,7 Тираж 171 экз. Заказ 46
Индекс 3649

Отпечатано в ИТЭФ, 117259, Москва, Б. Черемушкинская, 25